PRAMANA
— journal of
physics

Vol. 80, No. 4
April 2013
pp. 701–711

Induced moment due to perpendicular field cycling in trained exchange bias system

AMITESH PAUL[1,*] and S MATTAUCH[2]

[1]Technische Universität München, Physik Department E21, James-Franck-Strasse 1, D-85748 Garching b. München, Germany

[2]Jülich Centre for Neutrom Science Forschungszentrum Jülich GmbH, Außenstelle am FRM-II c/o TU München, Lichtenbergstraße 1, D-85747 Garching b. München, Germany

*Corresponding author. E-mail: amitesh.paul@frm2.tum.de

MS received 7 May 2012; revised 25 September 2012; accepted 8 October 2012

Abstract. Depth-sensitive polarized neutron scattering in specular and off-specular mode has recently revealed that perpendicular field cycling brings about a modification in the interfacial magnetization of a trained exchange coupled interface. We show here by various model fits to our neutron reflectivity data that a restoration of the untrained state is not possible in the case of our polycrystalline multilayer specimen. This is due to the magnetic moment at the interface induced only after perpendicular field cycling, changing the initial field-cooled state.

Keywords. Neutron reflectometry; magnetic properties of interfaces.

PACS Nos 61.05.fj; 75.70.Cn

Interfacial exchange coupling between a ferromagnet (FM) and an antiferromagnet (AF) can 'lock' the magnetization into the FM in a well-defined direction. This effect, which in a phenomenological picture takes the form of a unidirectional magnetic anisotropy, is known as exchange bias [1]. A cooling field H_{FC} (cooling below the ordering temperature of AF) essentially determines the state of the FM which in turn determines the strength of the bias field H_{EB} [2–4].

This exchange biasing demands a complete understanding [5] of various other related phenomena, such as coercivity enhancement [6,7], asymmetric hysteresis loops [2] and last but not the least, the training effect [8]. Difference between subsequent (partial) magnetization reversal loops is called the 'training effect'. Even though the microscopic origin of the training effect is still under debate, it is generally agreed to be due to the rearrangement of interfacial AF spin structure, which can be considered as rotatable hysteretic grains (rotatable anisotropy) particularly in polycrystalline specimens [9,10].

Generally, a relatively large training is seen between the first and second hysteresis loops (and a comparatively small effect for the subsequent higher number of loops). The

strong training behaviour between the first and second hysteresis loops is usually attributed to some initial non-equilibrium arrangement or metastable state of the AF spins. The exact mechanism for the initial AF spin arrangement is under debate.

Brems *et al* [10] attempted to restore the untrained state. In their case the initial cooling field was applied sufficiently higher than the saturation field which in such circumstances shows normal training. After two sequential field cycles, for a moderate magnetic field, applied perpendicular ($\perp^r$) to the cooling field, they could affect the interfacial magnetization of the AF grains thereby regain the asymmetry and claimed for the restoration of the untrained state that was lost after the initial field cycles. In fact a very similar phenomenon was reported earlier by the same group on stripes of CoO/Co as well [11], the only difference being the strength of the cooling field that may determine the degree of asymmetry in reversal in the latter version.

Very recently we reported that such a restoration of the untrained state may not be possible as an extensive modification of the initial field-cooled state of the interface had been realized after perpendicular field cycling [12]. In this paper we provide a deeper and elaborate analysis of the neutron reflectivity data with various model fits for confirming our observation.

Depth-sensitive neutron scattering under grazing incidence with polarization analysis (PNR) [3,13] were used for our investigation on a microscopic scale. In the experiment four different cross-sections can be distinguished, namely non-spin flip (NSF): (R_{++} and R_{--}) and spin flip (SF) channels (R_{+-} and R_{-+}). Here $+$ and $-$ signs are used to distinguish the intensity contributions R representing a polarization component parallel or antiparallel to the guiding field, respectively. $R_{++/--}$ contains the sum/difference between the nuclear and magnetic scattering, whereas the SF signal contains only the magnetic information.

The NSF scattering amplitude provides information about $\rho_n \pm \rho_m \cos \phi_A$, and SF the information about $\rho_m^2 \sin^2 \phi_A$, if the domain size is larger than the projection of the neutron coherence length along the sample plane ($l_\parallel$). Here ϕ_A is the angle between the direction of the induction vector $\vec{B}$ and the neutron spin quantization axis (if the neutron polarization vector is directed along the guide field which is also applied to the sample then, ϕ_A can be considered as the angle between the magnetization M and the applied field H_a), which may not be collinear with the applied field.

We have investigated multilayers of the composition SiO_2/[Co(11.0 nm)/CoO(3.0 nm)/Au(25.0 nm)]$_{16}$ with different sequential field-cycles [8]. Microstructural characterization has been done using cross-sectional transmission electron microscopy (XTEM). The neutron scattering experiments were performed using the polarized neutron reflectometer with polarization analysis V6 at the BER-II for a wavelength of [4.66]Å and at TREFF at FRM-II for a wavelength of [4.73]Å, measuring the specular and off-specular data simultaneously. All measurements were done after the sample was cooled to 10 K from room temperature (RT) by a closed-cycle refrigerator in the presence of a defined cooling field provided by an electromagnet.

Figure 1 shows the sketch of the direction of the magnetic fields during the filed cycles and the scattering geometry. Here H_a is the applied filed which is shown to be antiparallel to the cooling field H_{FC}, K_{ud} indicates the unidirectional anisotropy direction (opposite to the cooling field direction) and M_{FM} is the FM magnetization. The perpendicular field $H_\perp$ is also shown (perpendicular to H_{FC} in the sample plane).

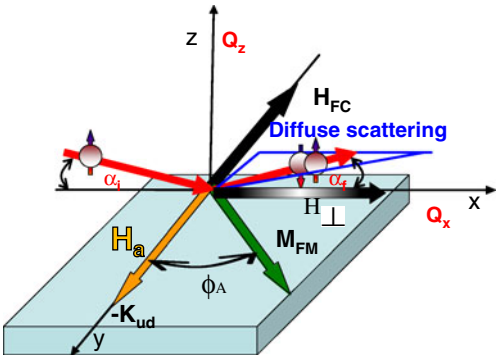

Figure 1. Illustration of the different in-plane anisotropy axes and the scattering geometry. In this figure H_a is shown to be antiparallel to H_{FC}. Here K_{ud} indicates the unidirectional anisotropy direction. M_{FM} is the FM magnetization making an angle ϕ_A with respect to the field axis.

Transmission electron microscopy studies have been carried out on cross-sectional samples. Conventional diffraction contrast images in bright-field imaging mode were obtained. In figure 2, the layered structure with sharp interfaces shows the existence of columnar grains (≈15–20 nm) that are vertically correlated from layer to layer.

Initially the sample was field cooled at $H_{FC} = -4.0$ kOe and then it was subjected to two consecutive field cycling (first and second). This was followed by a field cycling ($H_{\perp}^{max} = 1750$ Oe) perpendicular to the initial cooling field before it was measured along the initial cooling field (third). The measurements were done after the third field cycle, i.e. during the fourth field cycle (which is along the same direction as the first and second field cycles). The field value for $H_{\perp}$ was chosen following the argument that beyond a certain

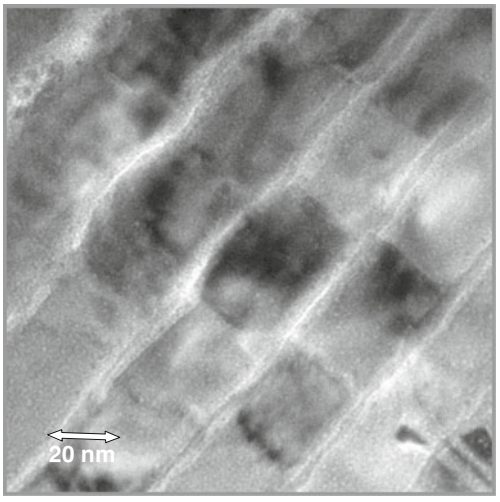

Figure 2. Cross-sectional TEM images showing vertical structural correlation.

field strength the AF moments would have undergone a completely new arrangement (much different from the initial direction) [11].

Figure 3 shows the hysteresis loops measured using a superconducting quantum interference device (SQUID) for an in-plane cooling field and longitudinal magnetization measurements at 10 K for the sample. Clearly seen is the usual asymmetry in the magnetization reversal and the disappearance of the asymmetry after the first field cycle. The room-temperature (RT) data show that the saturation field is around 100 Oe. We point out that the exchange bias field along the cooling field axis is estimated to be around −700 Oe.

A detailed description of the technique and measurements can be found in ref. [14]. In specular scattering geometry, the normal wave vector transfers $q_\perp = (2\pi/\lambda)[\sin(\alpha_i) + \sin(\alpha_f)]$ are probed while off-specular scattering contributions along the in-plane momentum transfer vector $q_\parallel = (2\pi/\lambda)[\cos(\alpha_f) - \cos(\alpha_i)]$ arise, when the in-plane translational symmetry is broken by interface waviness (roughness) or by magnetic domains on a length scale shorter than the neutron coherence length ($l_\parallel$) along $q_\parallel$. The non-spin flip (NSF) scattering amplitude provides information about $\rho_n \pm \rho_m \cos \phi_A$, and the spin flip (SF) channels measure $\rho_m^2 \sin^2 \phi_A$, if the domain size is larger than the projection of the neutron coherence length along the sample plane ($l_\parallel$). Here ϕ_A is the angle between the magnetization M and the applied field H_a (which is the neutron quantization axis).

We show the intensity maps (off-specular and specular NSF/SF scattering signals) measured at the reflectometer TREFF at FRM-II in figures 4a and b after the system is cooled down to 10 K in the presence of H_{FC}. The intensity along the diagonal $\alpha_i = \alpha_f$ is the specular reflection along $Q_\perp$. Vertical correlation of the structure is evident in the diffuse streaks across the Bragg peaks for the data measured at 4500 Oe (figure 4a). The state of the system when measured at the first reversal point is shown at around 1750 Oe (figure 4b). First reversal point is the point in the field axis where the magnetization is reversed for the first time after the sample is cooled in a field directed opposite to the applied field. This is also the coercive field along the decreasing branch of the hysteresis

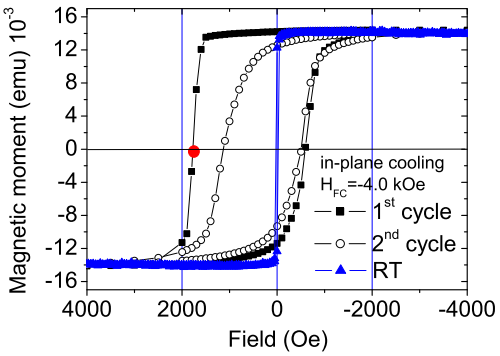

Figure 3. SQUID magnetization hysteresis loops for the sample for the two consecutive field cycles. The measurements were done at room temperature (triangles) and at 10 K (after cooling down in $H_{FC} = -4$ kOe). The first reversal point is shown in red as a dot. We do not show the measurement points after the perpendicular field cycle since the measurements could not be done in a SQUID.

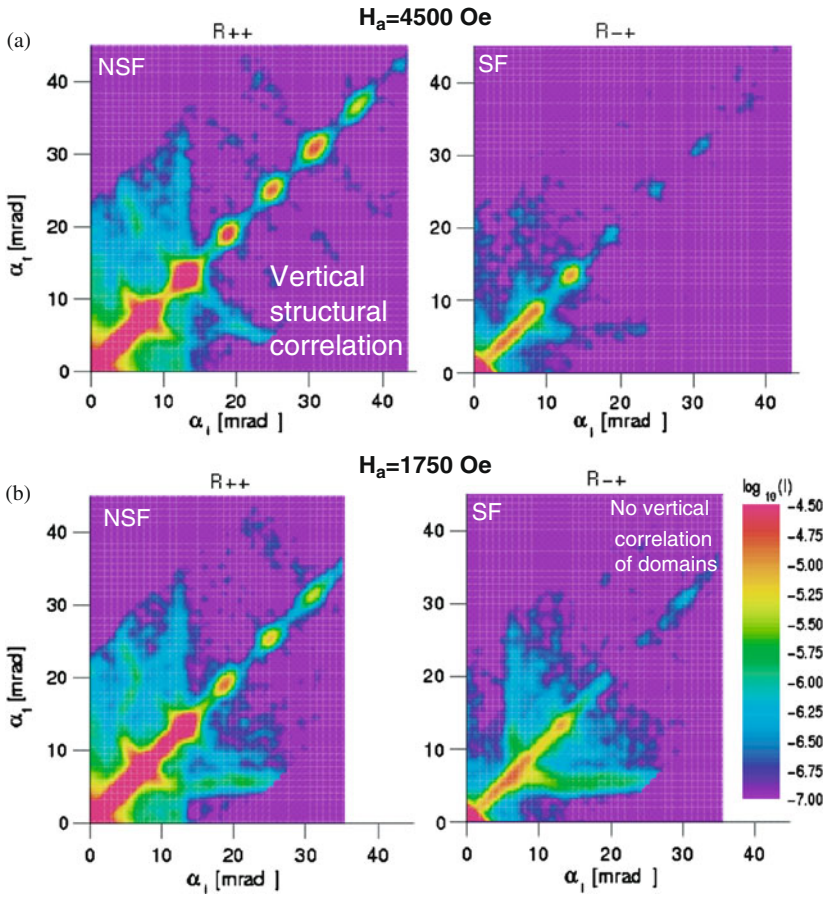

Figure 4. NSF and SF intensity maps [R_{--} and R_{+-}] from Co/CoO/Au ML measured on TREFF at two different applied fields (**a**) 4500 Oe and (**b**) 1750 Oe. The colour bar encodes the scattered intensity on a logarithmic scale.

loop (H_a antiparallel to H_{FC}). The V6 measurements were done at various fields 200 Oe, 1000 Oe, 1750 Oe and 4000 Oe and the TREFF measurements were done only at two specific fields 1750 Oe and 4000 Oe. At V6 we could measure only the specular reflectivities whereas at TREFF we could measure the intensity maps showing the specular as well as the off-specular intensities. All the preconditions for the two measurements (e.g. the cooling field and the perpendicular field) were kept very similar at the two instruments.

Note that the corresponding SF signal do not show the streaks when measured at 4000 Oe, indicating their non-magnetic origin. Instead, the laterally correlated magnetic scattering signal, related to domain size, can be seen in the SF signal measured close to the reversal point at 1750 Oe. At the reversal point the NSF intensities are divided into the two channels [$R_{++} \propto (\rho_n + \rho_m \cos \phi_A)$ and $R_{--} \propto (\rho_n - \rho_m \cos \phi_A)$] and hence may appear less prominent when compared to that measured at the saturation field (where most of the intensities are concentrated along the R_{++} channel as $\phi_A = 0$). Interestingly, these

domains remain vertically uncorrelated [12] even as the granular structure is vertically correlated, at least to some extent, when they are looked at macroscopically.

In figure 5 we plot the spin asymmetry (SA = $[R_{++}-R_{--}]/[R_{++}+R_{--}]$) from the specular reflectivity patterns of the specimen (reconstructed from ref. [12]) at various field values as indicated. The state of the trained specimen after the perpendicular field cycling (during the fourth field cycle) shown in figure 5 is measured at 200 Oe, 1000 Oe, 1750 Oe and finally at 4000 Oe. When compared to the profile measured at RT, the main difference that one can see is that the net magnetization is reversed only after 200 Oe of applied field as the coercive field has been estimated at around 700 Oe. The reversal is clear following the reversal of the positions of the Bragg peaks (arrows) with respect to the zero axis level of the SA. Surprisingly, another and more significant difference in the profile is seen around the third-order multilayer peak ($0.048 \leq Q \leq 0.058$) as its intensity is drastically reduced in comparison to that when it was measured at RT (open circle). Note that all the reflectivity patterns were measured at the reflectometer V6, with very similar measuring conditions such as polarizer and flipper efficiencies, similar background level and so on. Thus, their relative intensity variations can be easily compared.

Model fit to the data reveals that an increase of magnetism (comparable to $\rho_{\mathrm{m-Co}} = 3.88 \times 10^{-6}\,\text{Å}^{-2}$) at the CoO–Co interface, within the CoO layer, has taken place within a length scale of ≈0.7 nm (∼2–3 monolayers). This increase is with respect to that at saturation at 10 K (where $\rho_{\mathrm{m-CoO}} = 0$). We give fitted parameters that were varied for different temperatures in table 1.

This induced magnetism into the AF layer is unique in its nature as it results from direct manipulation of the uncompensated moments at the AF–FM interface. Such manipulation obviously fails to restore the untrained state [10].

One may note that all the structural as well as magnetic properties are initially estimated for the saturated case (taking the case of non-ideal polarizing and analysing units). At all

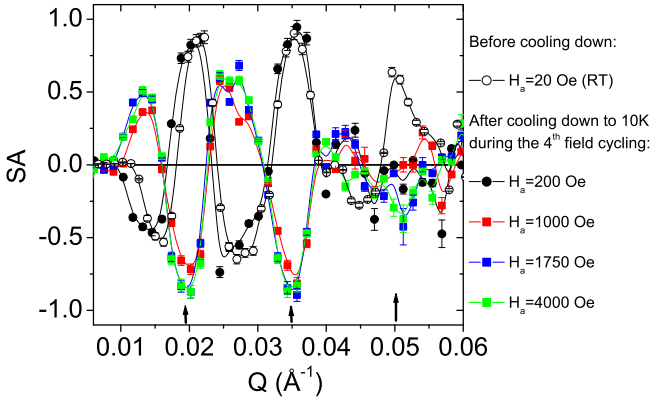

Figure 5. Spin asymmetry (SA) from NSF specular reflectivity patterns [R_{++} and R_{--}] from Co/CoO/Au ML at different conditions and measuring fields on the reflectometer V6. The data were reconstructed from ref. [12]. The positions of the multilayer Bragg peaks are indicated by black arrows. The measurements were done after the third field cycle, i.e. during the fourth field cycle (which is along the same direction as the first and second field cycles). The lines are guides to the eye.

Table 1. Thicknesses and scattering length densities of the specimen as obtained from the least square fits to the reflectivity data measured at different temperatures and fields.

Field of measurements	Thickness (nm) ±(0.3)	ρ_n ($Å^{-2}\times10^{-6}$) ±(0.02)	ρ_m ($Å^{-2}\times10^{-6}$) ±(0.02)	ϕ_A (°) ±(5)
RT at 20 Oe				
CoO	3.2	4.3	0.0	0
Co	10.8	2.2	3.88	0
10 K at 1750 Oe Model A: Induced magnetization in CoO				
CoO	2.5	4.3	0.0	0
Co–CoO	0.7	4.3	3.88	30
Co	10.8	2.2	3.88	30
10 K at 1750 Oe Model B: Intermediate layer				
CoO	2.5	4.3	0.0	0
Co–CoO	0.7	4.3	2.01	30
Co	10.8	2.2	3.88	30
10 K at 1750 Oe Model C: Magnetization in entire CoO				
CoO	2.5	4.3	2.01	0
Co–CoO	0.7	4.3	2.01	30
Co	10.8	2.2	3.88	30

the other fields we vary the magnetic properties to arrive at with our analysis regarding the magnetic state of the system. The resolution of the wavelength, the divergence of the beam and the illumination effects on the size of the sample are all convoluted with the simulation.

In order to make our interpretation unambiguous, we explore various possibilities/ scenarios that may have resulted in a similar change in the reflectivity profile.

(1) *Structural roughness*: It may be argued that a structural roughness of the same order (0.7 nm) may have caused an alloying like effect which may also suppress the third-order peak. Interestingly, an alloying effect would have resulted in an intermediate layer (with intermediate structural and magnetic properties) and this layer would have been at the cost of few monolayers from each of the adjacent layers thicknesses.

Interestingly, any structural parameter is intrinsic to the system and cannot be temperature- or magnetic field history-dependent. Therefore, such an intermediate layer model (which may have been realized during the growth of the sample) would have been also valid thereby manifested in the room temperature data as well as in the data measured at 10 K (after field cooling) [12]. One can easily figure out that this is definitely not the case as the third-order peak is not suppressed for the two situations but is only suppressed after the third field cycling. This is clearly an indication of the induced magnetism after the third field cycle.

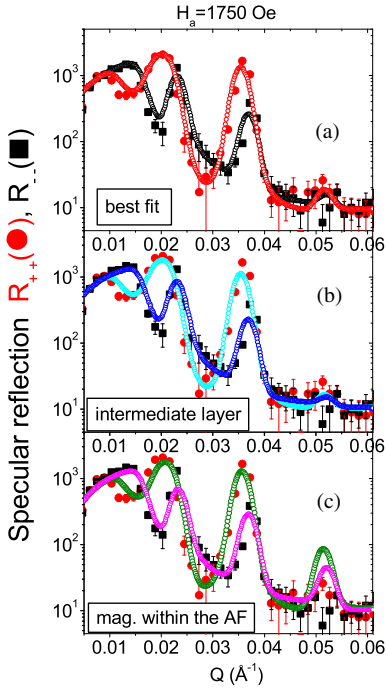

Figure 6. Plot of (**a**) experimental reflectivity data measured at 10 K during the fourth field cycle and the best-fitted pattern along with simulated pattern considering (**b**) an intermediate layer in the stack and (**c**) magnetization within the entire AF layer.

In our simulations we consider the situation of an intermediate layer (intermediate structural and magnetic properties of 0.7 nm) between AF and FM layers. From figure 6, one may argue that the two situations (considering and not considering the

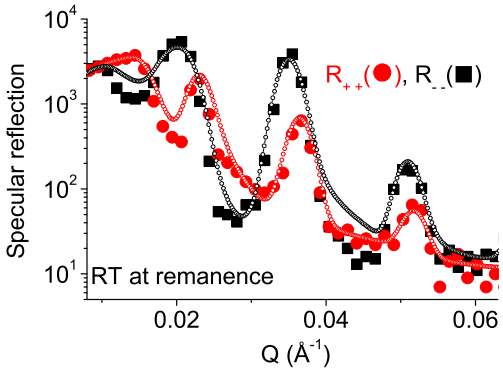

Figure 7. Plot of the experimental reflectivity data measured at RT at a remanence field along with simulated pattern.

intermediate layer) are difficult to compare as they are pretty close to each other. However, based on our argument in the last paragraph with reference to the RT data, one can be confident that the changes are not due to the existence of any intermixed layer. Figure 7 shows the reflectivity pattern measured at RT at a remanence field on the same reflectometer. The fits to the data are done according to the model shown in table 1.

(2) *Homogeneous magnetization within CoO*: In the second scenario, where an induced magnetism only at the interface was claimed [12], it can be doubted that the magnetism may have been extended throughout the entire thickness of the AF layer. Arguably, this would also have caused a reduced third-order multilayer peak.

We argue that in that case we would not have obtained any exchange coupling as then the entire CoO layer would have been behaving as a FM layer. However, an exchange coupling of 686 Oe has been observed [12]. This categorically indicates that the entire AF layer has not been affected due to the perpendicular field cycling but was restricted only at the interfaces.

Here also we check for a situation by considering an induced magnetism within the entire AF-block (the magnetization being lower than that of FM) and not residing only at the interface. One can see that this consideration also fails to reproduce our best-fit situation (the difference here is more drastic, especially around the third-order peak which is around $Q = 0.052\,\text{Å}^{-1}$). This has been clearly shown in figure 6.

(3) *Local canting due to perpendicular field*: In the third possible scenario, some canting of local magnetic moments towards magnetic field applied perpendicular to the AF axis may also induce magnetization within the AF layer. It may be argued that the exchange coupling to a FM may cause a dramatic enhancement of the effective field due to such canting. However, we can disregard this possibility simply because the suppression of the third-order peak is quite evident even at sufficiently large applied fields (e.g. 1750 Oe) which is very close to the saturation state of the system. At such a field we do not expect any canting to persist even if we may think of them to exist at lower fields. Thus, it can be stated that the suppression of the third-order peak is not due to any such local canting but due to the rearrangements of interfacial spins inducing magnetism within the AF layer.

Within the Fulcomer–Charap model [15], FM magnetization exchange couples with multiple AF grains with rotatable (responsible for training) and/or non-rotatable (responsible for bias field) moments but without any direct exchange coupling between the grains. Following the conjecture that exchange bias can involve aspects of glassy behaviour [16,17], some FM order at the surface of AF grains (below the superparamagnetic limit) can explain the field-induced magnetism. It is only above a critical value of the energy barrier per unit grain area of the AF (E_{AF}), that a portion of the AF grains are stable against reversal by the exchange field as the FM layer changes sign and contribute to H_{EB}. Now with a decrease in effective AF layer thickness, E_{AF} is also lowered, which in turn reduces the coercive field [12].

It may however be noted that a complete restoration of the untrained state and/or of the domain configuration of the CoO layer was not achieved and only partial reinduction was claimed by Brems *et al* [10]. Velthuis *et al* [18] performed measurements on Co/CoO

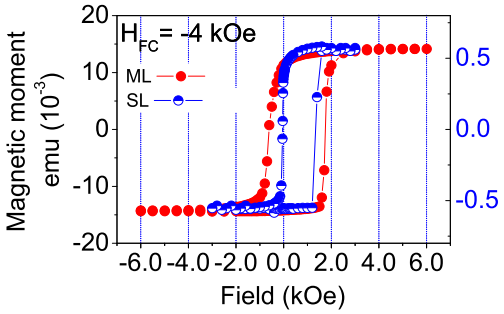

Figure 8. SQUID hysteresis loops for SL and ML after field cooling at $H_{FC} = -4.0$ kOe.

bilayers with field applied perpendicular to cooling field direction directly after field cooling and found that only within moderate applied fields was the rotation of magnetization reversible, while if going to higher field, it was not reversible. The angular variation (ϕ_A) of the net magnetization, as deduced from the fits to the specular reflectivity patterns [12], indicates that the reversal mechanism is predominantly via the uniform way (via rotation). The SF signals after the third field cycle has been predominantly above the level to that is expected for a non-uniform reversal. Note that a non-uniform reversal is expected for the decreasing branch in order to account for any partial asymmetric reversal.

The fact is that it is extremely difficult to prepare two bilayer samples that show the restoration of the untrained state for exactly the same amplitude of the applied perpendicular field. The reason is that the restoration is dependent on the microscopic antiferromagnetic domain distribution, which is difficult to control. In this regard we would like to state that the interfacial state of a bilayer (SL) from that of a multilayer (ML) can be made very similar for our samples [4]. We present a comparison in figure 8 of the magnetization behaviour of a bilayer and that of a multilayer measured in a SQUID. The sharpness in reversal (in the decreasing branch: opposite to the cooling field) indicates that the interfaces are indeed similar. However, it can still be argued that the growth of the bilayers on top of each other, separated by a 25 nm thick Au layer (as in the present case), will probably have an influence on the antiferromagnetic domain structure which would then may be difficult to compare exactly [19].

In summary, we confirm that an in-plane magnetic field cycling, perpendicular to the cooling direction, neither restores the untrained state nor the asymmetry in reversal in our multilayered sample. It only redefines the state of interface. With various model fits to the PNR data we argue that only an extra interfacial magnetism can explain the measured data.

Acknowledgement

The authors would like to thank Ulrike Bloeck for the assistance in TEM measurements.

References

[1] W H Meiklejohn and C P Bean, *Phys. Rev.* **102**, 1413 (1956)
[2] M Gierlings, M J Prandolini, H Fritzsche, M Gruyters and D Riegel, *Phys. Rev.* **B65**, 092407 (2002)
[3] A Paul, E Kentzinger, U Rücker and Th Brückel, *Phys. Rev.* **B73**, 092410 (2006)
[4] A Paul, D Bürgler, M Luysberg and P Grünberg, *Europhys. Lett.* **68**, 233 (2004)
[5] G Scholten, K D Usadel and U Nowak, *Phys. Rev.* **B71**, 064413 (2005)
[6] M D Stiles and R D McMichael, *Phys. Rev.* **B59**, 3722 (1999)
[7] M Gruyters and D Schmitz, *Phys. Rev. Lett.* **100**, 077205 (2008)
[8] A Paul, E Kentzinger, U Rücker and Th Brückel, *Phys. Rev.* **B74**, 54424 (2006)
[9] A Paul, C M Schneider and J Stahn, *Phys. Rev.* **B76**, 184424 (2007)
[10] S Brems, Kristiaan Temst and Chris Van Haesendonck, *Phys. Rev. Lett.* **99**, 067201 (2007)
[11] Steven Brems, Dieter Buntinx, Kristiaan Temst, Chris Van Haesendonck, Florin Radu and Hartmut Zabel, *Phys. Rev. Lett.* **95**, 157202 (2005)
[12] A Paul, *Appl. Phys. Lett.* **97**, 032505 (2010)
[13] A Paul, E Kentzinger, U Rücker, D Bürgler and P Grünberg, *Phys. Rev.* **B70**, 224410 (2004)
[14] A Paul, *Pramana – J. Phys.* **78(1)**, 1 (2012)
[15] E Fulcomer and S H Charap, *J. Appl. Phys.* **43** (1972)
[16] A Paul and S Mattauch, *Appl. Phys. Lett.* **95**, 092502 (2009)
[17] M Gruyters, *Euro. Phys. Lett.* **77**, 57006 (2007)
[18] Te Velthuis *et al*, *J. Appl. Phys.* **87**, 5046 (2000)
[19] C V Haesendonck, private communication